Noname manuscript No.
(will be inserted by the editor)

Pixel lensing

Microlensing towards M31

S. Calchi Novati

Received: 2 November 2009 / Accepted: 20 November 2009

Abstract Pixel lensing is gravitational microlensing of unresolved stars. The main target explored up to now has been the nearby galaxy of Andromeda, M31. The scientific issues of interest are the search for dark matter in form of compact halo objects, the study of the characteristics of the luminous lens and source populations and the possibility of detecting extra-solar (and extra-galactic) planets. In the present work we intend to give an updated overview of the observational status in this field.

Keywords Gravitational lensing · M31 · dark matter

PACS 95.75.De · 98.56.Ne · 95.35.+d

1 Introduction

Following the original suggestion of Paczyński (1), (stellar) gravitational microlensing is by now an established and efficient tool of research. The original motivation has been the search for dark matter in Galactic halos in form of compact halo objects (MACHOs). Meanwhile microlensing probed to be a powerful tool also for the analysis of the characteristics of the (luminous) lens and source populations and, more generally, of the Galactic structure. The first lines of sight to be explored have been those towards the Magellanic Clouds and the Galactic centre (for an updated account see the review of Moniez (2)). Along this second line of sight, the current main field of application is the search for extra-solar planets (thoroughly discussed in the review of Dominik (3)).

As for the search of compact halo objects, the results obtained along the line of sight towards the LMC are non-conclusive. The MACHO collaboration

S. Calchi Novati
Dipartimento di Fisica "E. R. Caianiello", Università di Salerno, 84084 Fisciano, Italy and Istituto Nazionale di Fisica Nucleare, Sezione di Napoli, Italy.
E-mail: novati@sa.infn.it

claimed the detection of a MACHO signal from objects of $\sim$ 0.4 $M_\odot$ that would constitute a (Milky Way) halo mass fraction $f \sim 20\%$ (4; 5). On the other hand, the EROS group found no candidate events along this line of sight and put a rather stringent limit *upper* limit, $f < 0.1$, in the mass range of compact halo objects preferred by the MACHO results (6). More recently, the OGLE collaboration presented two candidate events towards the LMC out of their OGLE-II campaign, concluding that this is compatible with the expected self-lensing signal (7).

As soon as one wants to move beyond these nearby targets a difficulty arises in that the potential sources of microlensing events are no longer resolved objects and we enter the regime usually referred to as *pixel lensing*. (At even larger distance we enter the realm of quasar, or cosmological, gravitational microlensing, which is the subject of the review of Wambsganss (8).) Up to know the main field of application of pixel lensing has been the nearby Andromeda galaxy, M31.

Pixel lensing, and in particular the line of sight towards the Andromeda galaxy, is the subject of the present review. Many reviews exist on the subject of gravitational microlensing (e.g. Paczyński (9), Roulet and Mollerach (10), Wambsganss (11)). The theoretical aspects related more specifically to pixel lensing have also been already thoroughly discussed in a number of papers. In the present work we intend to give an updated overview of the current observational status in this field. The outline is the following. We start with a brief discussion of the basic of pixel lensing, § 2. In § 3 we discuss M31 pixel lensing: we trace back the theoretical developments, § 3.1, and the observational campaigns carried out along this direction, § 3.2. The modelling of M31 is discussed in § 3.3 and the expected lensing signal in § 3.4. The main focus of the present review is on the presentation of the observational results obtained up to now along this line of sight, their interpretation and the outlook for future developments. This is the object of § 3.5. In particular we present the candidate events in § 3.5.1 and the results obtained on the MACHO content in § 3.5.2. In § 3.6 we discuss a further relevant scientific application, the search for extra-solar planets in M31 with pixel lensing. Finally, in § 4, we discuss the application of pixel lensing towards targets beyond the Local Group.

2 Basic of Pixel lensing

Pixel lensing is gravitational microlensing of unresolved stars (12). Looking for microlensing events, and moving beyond the more nearby available targets (the Galactic bulge and the Magellanic Clouds) the potential sources are no longer resolved (though possibly blended) objects[1]. This establishes the difference with respect to "classical" gravitational lensing. The key idea in this regime is therefore to look for flux variations of the picture elements of the image (the pixels). The appealing part of this approach is, besides the possibility

[1]Because of blending, often the resolved microlensing sources are referred to as "objects" rather than "stars".

to explore more distant targets, the huge increase of potential sources (all of them, more over, accessible to within rather small field of views compared to local searches). The related problem is the impossibility, in most cases, to access the source star flux. In turn, this enhances a series of problems in the analysis peculiar to pixel lensing.

Quite generally, we may write the light curve flux for a microlensing event as

$$\Phi\left(t,\{\theta\}\right)=\Phi^{*}\cdot\left(A\left(t,\{\theta\}\right)-1\right)+\Phi_{\mathrm{B}}\,. \tag{1}$$

Here Φ^{*} is the flux of the unlensed source, $A\left(t,\{\theta\}\right)$ is the microlensing amplification, with $\{\theta\}$ being the amplification parameters, and Φ_{B} the *background* flux level. The microlensing amplification in the simplest (and standard) situation of point source, point lens and uniform relative motion depends on three parameters: the impact parameter, u_0, the time of maximum amplification, t_0, and the Einstein time, t_{E} (the corresponding light curve is usually referred to as *Paczyński* light curve):

$$A\left(t,\{\theta\}\right)=\frac{u^{2}+2}{u\sqrt{u^{2}+4}}\,, \tag{2}$$

where

$$u\equiv u\left(t,\{\theta\}\right)=\sqrt{u_{0}^{2}+\left(\frac{t-t_{0}}{t_{\mathrm{E}}}\right)^{2}}\,. \tag{3}$$

The relevant physical parameter is t_{E} which sets the fundamental timescale of the event. It depends from the lens *mass*, M, the most relevant physical information one is interested into, and other usually non directly observable quantities as the lens and source distances, D_{l} and D_{s} respectively, and the lens relative velocity v with respect to the line of sight, as $t_{\mathrm{E}}=R_{\mathrm{E}}/v$. R_{E} is the Einstein radius, and $\theta_{\mathrm{E}}=R_{\mathrm{E}}/D_{\mathrm{l}}$ the angular Einstein radius (on the lens plane)

$$\theta_{\mathrm{E}}=\sqrt{\frac{4GM}{c^{2}}\frac{D_{\mathrm{s}}-D_{\mathrm{l}}}{D_{\mathrm{l}}\,D_{\mathrm{s}}}}\,. \tag{4}$$

θ_{E} is the fundamental (angular) length scale which sets the cross-section of microlensing events.

In the "classical" lensing regime the quantity $\Phi(t)$ in Eq. 1 is the measured flux from the lensed object. With $A(t)\rightarrow 1$ for $|t|\gg t_0$, the background level reads $\Phi_{\mathrm{B}}=\Phi^{*}+\Phi'_{\mathrm{B}}$, with Φ'_{B} being the flux of any unlensed source blended within the source star PSF. In principle Φ'_{B} is a well known quantity so that the microlensing light curve can be fitted to the four unknown parameters t_{E}, u_0, t_0 and Φ^{*}[2].

[2]From the observational point of view the situation, however, is not as straightforward as the actual blending fraction may not be as easy to be determined. In fact, for microlensing analyses towards the Galactic bulge, a robust agreement between theoretical expectations and observational results has been reached only for a restricted sample of selected bright, standard candle, sources for which blending can be actually assumed to be negligible (13; 14; 15). Also for LMC analyses blending is a particularly delicate issue to be dealt with (4; 6; 7).

In the pixel-lensing regime, instead, the quantity $\Phi(t)$ in Eq. 1 is the *pixel* flux. Within the same pixel there is a large number of potential sources, and an even much larger number of stars too faint to give rise to any detectable lensing signal. This can be looked at as the opposite case of classical lensing, namely, a completely blended situation with $\Phi'_{\rm B} \gg \Phi^*$. As an immediate consequence the photon *noise* is going to be dominated by the underlying background of the unresolved sources rather than from the actual star being lensed (and in particular of the amplification). This is the characteristic signature of pixel lensing analyses. A related issue is the *threshold* magnification needed to give rise to a detectable signal that we are going to detail below. As a direct consequence we may expect to be difficult to measure from a light curve fit to the data the unlensed flux and the event timescale, $t_{\rm E}$. In fact, one usually finds a strong degeneracy in the parameter space $t_{\rm E}$, u_0 (or, equivalently, Φ^*, u_0) (16). A possible way out is that of reducing the number of free parameters from three to two Φ_*, u_0, $t_{\rm E} \rightarrow \Delta\Phi$, $t_{\rm FWHM}$ (16; 17). Both the new parameters $\Delta\Phi$ and $t_{\rm FWHM}$ can always be easily measured on the light curve as the flux difference at maximum amplification and the full-width-half-maximum event duration, respectively. The FWHM timescale, $t_{\rm FWHM}$, is proportional to the Einstein timescale, $t_{\rm FWHM} = t_{\rm E} \cdot f(u_0)$ (17). For large values of the amplification, $u_0 \ll 1$, this relationship reduces to $t_{\rm FWHM} = \sqrt{12} u_0 t_{\rm E}$.

Gould (12) made the further distinction, within the pixel-lensing regime, of a "semiclassical" regime, where one can yet get to break the parameter degeneracy and evaluate the unlensed source flux, and a "spike" regime, where the background level is so large that only events with extremely large amplification, $u_0 \ll 1$, are observable, and where it is actually impossible to determine the physical duration $t_{\rm E}$.

As remarked by Gould (12), M31 pixel lensing is at the limit between the semiclassical and the spike regime. It is not obvious to, but sometime possible to measure out of the observed light curves, with a reasonable precision, the physical timescale $t_{\rm E}$. To this purpose, an extremely good sampling along the flux variation, and in particular along their wings (12; 18; 19), is essential. Besides, a suitable sampling is in order also to distinguish lensing signals from intrinsic variable objects. As a note of terminology, therefore, we may say that a "pixel-lensing" event, besides the access to the knowledge of the source flux, is a microlensing event for which the photon noise is dominated by that of the background level.

In the classical regime a microlensing event is considered to be enhanced whenever the impact parameter, u_0, gets smaller than one. For a specific experimental campaign this value may be chosen to be somewhat smaller or larger, but in any case it is a fixed quantity whatever, in particular, the source flux value. In the pixel lensing regime the situation is altogether different. The threshold impact parameter, $u_{\rm T}$, is determined given the, line of sight dependent, background noise and depending on the underlying source luminosity function (20). In particular it turns out that, typically, $u_{\rm T} \sim \mathcal{O}(10^{-2} - 10^{-3})$.

To conclude, before moving to applications of pixel lensing towards M31 and even more distant targets, we note that pixel lensing can in fact be used

also for *nearby* targets. In particular, microlensing analyses towards the LMC are usually carried out looking at resolved objects, but one can expect microlensing events also from unresolved LMC sources (in fact, as it turns out, more events than from just resolved objects). Such a programme has been carried out using a part of the EROS-1 data towards the LMC bar (21; 22).

3 M31 pixel lensing

3.1 Theoretical developments

The idea of looking for microlensing events with sources (and lenses) belonging to M31 has been first, independently, proposed by Crotts (23) and Baillon et al. (24). Crotts (23) first acknowledged the opportunity given by the geometry of M31, the inclination of the M31 disk, to get a signature in the spatial distribution of microlensing events due to M31 compact halo objects. Furthermore, he considered, as a possible detection method, a first idea of what was going to become the scheme of *difference image photometry* (25). On the other hand, the main focus of the analysis presented by Baillon et al. (24) has been on the acknowledgement of the role played by looking for microlensing events due to unresolved stars. As discussed in the previous Section, this introduces additional difficulties in the analysis but, on the other hand, translates in an appealing substantial increase into the number of potential sources. Furthermore, they have presented a first, detailed, Monte Carlo simulation framework to establish the expected signal for a microlensing experiment. In particular they have shown the relevant result that we may expect the sources of most events to be bright stars (as a typical value, roughly $M_V < 2$) with not so large amplification, and not, therefore, faint sources with extremely large amplification. Furthermore, following this first analysis, an original scheme of light curve analysis, the *superpixel photometry* (26; 22)[3] was then developed. Shortly after, Jetzer (27) presented a more detailed theoretical study on gravitational microlensing towards M31 with emphasis on the relevant microlensing quantities, the *optical depth* and the *microlensing rate*.

A further advantage of the line of sight towards M31 for MACHO searches, whose relevance can not be stressed enough, is the possibility, looking at it from outside, to fully map the M31 own dark matter halo. Such an analysis is not possible for the Galactic halo.

These first theoretical analyses have been thoroughly developed. Colley (28) have formalized the problem of detecting events through the "threshold" approach. Han (29) analysed the problem of observations towards the M31 bulge evaluating the optical depth, the timescale distribution and the expected

[3]Difference image analysis and superpixel photometry are still the two currently used photometry analysis schemes for pixel lensing observations. In fact these two methods are not mutually exclusive, in that a possible, and perhaps suitable strategy, would be to use the superpixel photometry approach for the identification of flux variations, and then make use of the more refined difference image photometry only on a subset of selected light curves.

event rate for a specific observational set up. Furthermore, he provided an important result on the extinction by the dust in the M31 disk. Gondolo (17) considered the problem of evaluating the optical depth in the pixel lensing regime, namely, by making use of the FWHM timescale, $t_{\rm FWHM}$, rather than the Einstein timescale, $t_{\rm E}$. Further analyses concerning the optical depth and the event rate for M31 pixel lensing have been carried out by Gyuk and Crotts (30) and by Baltz and coauthors (18; 31; 32).

A crucial aspect of any microlensing campaign is the estimate of the expected signal. Kerins et al. (20) outlined a detailed scheme for a pixel lensing simulation. Riffeser et al. (33) presented a thorough analysis of the theory and application of microlensing towards M31. The scheme of the Monte Carlo simulation first sketched in (24; 26) has been further discussed by Calchi Novati et al. (34; 35).

3.2 Observational campaigns

Following, and parallel, to these theoretical developments, several observational pixel-lensing campaigns have been undertaken towards M31. The theoretical analyses of Crotts lead to the Vatican Advanced Technology Telescope[VATT]/Columbia campaign (36; 37), using data from the 1.3m Vatican telescope and the MDM 1.3m telescope and to its successor, the MEGA (Microlensing Exploration of the Galaxy and Andromeda) collaboration who used the 2.5m INT (Isaac Newton Telescope) (38; 39). The work of Baillon et al. (24) led to the formation of the AGAPE (Andromeda Galaxy and Amplified Pixels Experiment) collaboration[4] who used the 2m TBL (Telescope Bernard Lyot) (26; 40). As a part of this same project, within the SLOTT (Systematic Lensing Observations at Toppo Telescope)-AGAPE collaboration, Calchi Novati et al. (41; 42), thanks to a collaboration with A. Gould and sharing data with the VATT/Columbia project, analysed data collected at the 1.3m MDM telescope. Still from a collaboration with the AGAPE group, the Nainital group carried out a campaign with the 104cm Sampurnanad telescope (43). Eventually, from the AGAPE experiment, the POINT-AGAPE (Pixel-lensing Observations with the Isaac Newton Telescope) collaboration was begun sharing data collected at the 2.5m INT telescope with the MEGA collaboration (44; 45; 46; 34). Finally, the WeCAPP (Wendelstein Calar Alto Pixellensing Project) group carried out a several-years campaign using both the 1.3m Calar Alto telescope and the 0.80m Wendelstein telescopes (47; 48). In Table 1 we resume the present status. Most observational campaigns have been observing around the M31 bulge region, although usually avoiding the very M31 centre. In Fig. 2 we draw the contours of the field observed by the POINT-AGAPE/MEGA collaborations, up to now the pixel lensing observational campaign that covered the largest field of view.

Ongoing microlensing campaigns are trying to overcome some of the problems of the first campaigns. E. Kerins et al. (50) started the ANGSTROM

[4] A brief history of the beginning of the AGAPE collaboration is given in the Appendix.

Table 1 Completed and ongoing microlensing campaigns towards M31. Fifth column: number of microlensing candidate events, in bracket those that are no longer considered as such (see text for details) and in particular not reported in Table 2 and in Fig. 2.

collaboration	years	telescope	f.o.v.	# events	ref
VATT/Columbia	1997	1.8m VATT	$2 \times (11.3' \times 11.3')$	(3)+3	(36; 37)
	1997-1999	1.3m MDM	$2 \times (17' \times 17')$		
MEGA	1999-2002	2.5m INT	$2 \times (33' \times 33')$	(4)+14	(38; 39)
AGAPE	1994-1996	2.0m TBL	$6 \times (4.5' \times 4.5')$	1	(26; 40)
SLOTT-AGAPE	1997-1999	1.3m MDM	$2 \times (17' \times 17')$	(5)+3	(41; 42)
POINT-AGAPE	1999-2001	2.5m INT	$2 \times (33' \times 33')$	7	(44; 49; 45; 46; 34)
WeCAPP	1997-2008	1.23m CA	$17.2' \times 17.2'$	2	(47; 48)
		0.80m We	$8.3' \times 8.3'$		
Nainital	1998-2002	1.04m Sa	$13' \times 13'$	1	(43)
ANGSTROM	2004-	2m LT & FTN	$4.6' \times 4.6'$	-	(50)
PLAN	2006-	1.5m OAB	$2 \times (13' \times 12.6')$	2	(51; 35)

(Andromeda Galaxy Stellar Robotic Microlensing) collaboration to probe stellar lensing in the inner bulge region of M31 down to low mass stars with the specific aim to constrain the 3d structure of the M31 bulge. By making primarily use of a network of 2m class robotic telescopes with a small field of view, $4.6' \times 4.6'$, centered right in the M31 centre (the Liverpool Telescope, LT, and the Faulkes Telescope North, FTN), plus 3 additional telescopes (the 1.8m Bohyunsan Observatory in Korea, the 2.4m Hiltner MDM at Kitt Peak, US, and the 1.5m Maidanak Observatory in Uzbekistan), the ANGSTROM collaboration has also undertaken the first ambitious and challenging project of real time microlensing discovery outside the Galaxy: the APAS, the Angstrom Project Alert System (52). In particular they also considered the possibility to use this high cadence survey to flag and follow up binary systems in M31 (53). The ANGSTROM project has begun taking data in 2004. The PLAN (Pixel Lensing Andromeda) collaboration undergone a new observational campaigns making use of the 1.5m Loiano Telescope at OAB (Astronomical Observatory of Bologna, Italy) (51). With a CCD field of view of $13' \times 12.6'$ they have been monitoring two fields around the inner M31 region, with an aggressive observational strategy of consecutive and full nights. Given the short duration of the expected events, a good sampling is essential first to safely distinguish microlensing events from intrinsic variables and then to robustly characterize the detected events. The PLAN collaboration started observing with a pilot season campaign in 2006, and is still currently carryng on his observational effort. In particular they have reported the detection of 2 microlensing candidates from their 2007 season (35). In 2008 they begun using also the 1.5m TT1 telescope (Astronomical Observatory of Capodimonte, Napoli, Italy).

Both these ongoing observational campaigns suffer, in the perspective of the search for MACHOs, from an intrinsic limitation in that their observed fields of view are rather small. As we will detail later, the spatial distribution of the lensing events is an important issue, so that the possibility to monitor not only the M31 central region is crucial for a correct understanding of the lensing signal. The PAnandromeda project[5] plans to make use of the 1.8m PS1 telescope[6] with a huge field of view of 6.4 sqdeg (with an almost complete 64×64 array of CCD devices, each about 600×600 pixels and using the "orthogonal transfer" technique for the read out). This will cover in a single shot all of the M31 field. M31 is expected to be monitored with a cadence of nightly exposures (such a tight sampling is extremely important, indeed essential, to cope with the expected flux variations lasting a few days only) of 12m and 6m in r' and i' band, respectively, for about 10 weeks per season (this overall exposure time per night, however, given the mirror size, may not allow to go fainter than previous campaigns, in particular the INT one which, with a 2.5m telescope, observed each field, usually, about 20m per night in r' band, though with a much more irregular sampling). Such an ambitious project is expected to bring extremely exciting results on M31 pixel lensing. The observational campaign has been started in 2009.

3.3 Modelling of M31

A correct modelling of M31 is an essential ingredient for any analysis aiming at describing the expected lensing signal along this line of sight. The starting point is an accurate model for the luminous components responsible for the expected self-lensing signal. This is particularly delicate also because, opposite to the LMC case, this signal, at least in the central M31 region, is in fact comparable to the would be MACHO signal.

M31 lies at a distance estimated at $\sim$ 785 kpc (54) (see also (55) who proposed a somewhat larger value), with a sharp inclination angle of 77° (56). The morphology of M31 is similar to that of the Milky Way, with a central bulge and a disc. The single one fundamental physical parameter linked to the expected lensing signal is the overall *stellar* mass of these luminous components. As for the bulge mass the estimate of Kent (57) of $4.0 \times 10^{10} M_\odot$ (for which a distance to M31 of "only" 690 kpc was used) has become a sort of "standard" reference value for most microlensing analyses (30; 20; 31; 33; 35). Together with a disc mass of $3.1 \times 10^{10} M_\odot$ (20; 33; 34; 35) this gives an overall M31 stellar mass of $\sim 7 \times 10^{10} M_\odot$. For their POINT-AGAPE analysis, however, Calchi Novati et al. (34) used, as a fiducial value, a lighter bulge of $1.5 \times 10^{10} M_\odot$, and the Kent (57) value as a test model only. Finally, de Jong et al. (39), for their MEGA analysis, used, for their fiducial model, 4.4 and 5.5 (in units of $10^{10} M_\odot$) for the bulge and the disc mass, respectively. On the other hand, most non-microlensing analyses usually get to a somewhat larger

[5] S. Seitz, talk given at the 13th Microlensing Workshop, 2009, Paris.

[6] http://pan-starrs.ifa.hawaii.edu/public/

overall stellar mass, $\sim 10 \times 10^{10} M_{\odot}$, but with a smaller bulge mass. In particular bulge and disc mass values are reported to be (in units of $10^{10} M_{\odot}$) 2.4 and 7.1 (58), 3.2 and 7.2 (59), 2.5 and 7.0 (60), 3.4 and 5.6 (61), 1.9 and 7.0 (62). Clearly there is still not a consensus on this issue. One leading reason is the uncertainty linked to the M/L ratio values and to the (related) issue of the internal M31 extinction (see also (63)). It is beyond our scope to enter a detailed discussion about this matter for which we refer to the previously cited works. We only note that, in particular for the bulge mass, the rather large value in microlensing analyses is usually assumed to be on the "safe" side in order not to underestimate the lensing bulge contribution. On the other hand, in microlensing analyses one should be careful to actually take into account the stellar mass contribution only, and this may be at odd with determinations based on dynamical grounds. Clearly, a correct estimate of the bulge and disc mass is essential in order to get to reliable estimates of the expected self-lensing signal.

For the overall bulge and disc structure the models are based upon the available surface brightness profiles. Besides the work of Walterbos and Kennicutt (56), we recall also the analyses of Kent (64; 65; 66) and in particular the bulge/disc decomposition discussed in (57) that have been taken as a basis, in particular, for many microlensing analyses (20; 34; 33; 35). Noteworthy, to discuss their microlensing results, de Jong et al. (39) made use of a fully self-consistent M31 model following the analysis of Widrow and Dubinksi (67). More detailed morphological analyses of the inner M31 bulge suggest also the presence of a bar-like structure (68; 69). A specific analysis on this issue from a microlensing perspective is given in Kerins et al. (50).

As for the bulge structure and population we finally mention the recent work of Saglia et al. (70) who present and discuss new optical long-slit data out to $5'$ from the M31 centre with the purpose to constrain the stellar and gas kinematics. In particular they point out that previous estimates of the velocity dispersion were severely underestimated and this lead them to revise upward, with respect for instance to the analyses in (60; 33; 58), the stellar mass of the bulge. Their analysis also suggests the possibility of an intrinsic triaxiality of the bulge and/or the presence of a bar.

A further, somewhat elusive, stellar component is the stellar halo of M31 (71; 72), known in particular to be rich in substructures (73; 74). The microlensing signal from this component may be expected to be enhanced because of the increase in the lens-source distance, however, because of the small density and overall total mass, one can expect that this should not be large with respect to microlensing events by lenses in the bulge or the disc. Anyway, a specific analysis on this issue still awaits to be carried out.

In order to specify a microlensing event one also needs the mass function for the lenses (given the overall mass of a lens component, this is related to the number of available lenses) and the luminosity function for the sources (given the surface brightness, this is related to the number of available sources along a given line of sight). We still lack definitive results on both these issues, even if the content of the M31 stellar bulge and disc have been already the

object of several analyses (75; 76; 77; 78; 79) (for the mass function we recall in particular the work of (80)). Therefore, most times Milky Way results (for the mass function) and synthetic luminosity functions are used (for microlensing-based analyses we refer for instance to the discussions in Riffeser et al. (33) and in Kerins et al. (50)). A relevant aspect to stress is that, whereas for the mass function one is mostly interested in the low mass tail, where most lenses are, for the luminosity function one is mainly interested in the opposite tail, the bright end, as one expect only giant stars as possible sources. Finally, one needs models for the velocity distributions (Ref. (70) and references therein) and the M31 transverse velocity (81).

In an early work, Braun (82), with a study of the neutral gas in M31, and in particular of the rotation curve out to 28 kpc, concluded on the lack of indications for a massive dark halo. This view is by now altogether changed. For instance, in a recent analysis, Chemin et al. (58), by studying the M31 rotation curve out to 38 kpc, conclude that the dark matter component is almost 4 times more massive than the baryonic mass. The authors also consider different shape for the dark matter halo, the Navarro-Frenk& White (83; 84) model, the Einasto model (85), and the (pseudo-)isothermal sphere. Noteworthy, these models all fail to exactly reproduce the observed rotation curve, and neither of them is found to be preferred.

3.4 The expected signal

A first characterisation of the expected pixel lensing signal may come from an analysis of the microlensing quantities, the optical depth and the microlensing rate. However, to properly address this issue a full simulation of a given experiment is needed. This holds because of the interplay among the background noise level, the threshold impact parameter and the luminosity function (more specifically, the exact fraction of unresolved stars that must be counted as possible sources) (20; 33; 50; 34; 35). In particular, a fundamental issue to be addressed is the correct understanding of the nature of the lenses. Either belonging to some known luminous population, for self-lensing events, or to the dark matter halo, for MACHO lensing. This is never trivial for microlensing events, as lens mass, lens and source distances and relative velocities are not directly measured. In the pixel lensing regime this is further complicated because of the additional degeneracy due to the ignorance of the source flux. Self lensing constitutes a background one must get rid of for the study of the MACHO lensing signal. Nonetheless, the self-lensing signal is relevant in itself. It allows one to assess the capability of one's pipeline to detect microlensing events, whenever expected, and, if possible, to "normalize" the expected self-lensing versus MACHO lensing signal. Furthermore, self lensing can also be used to study the characteristics of the luminous lens populations (for Galactic bulge observations we recall, for instance, the analysis of the bulge mass function in (86)).

At a first level of analysis three main statistics are available to characterize the lensing signal: the number of observed events, the duration and the distance from the M31 centre distributions. In principle, as for the spatial distribution, one might want to study the expected asymmetry for lensing events due to compact objects belonging to the M31 halo (Milky Way compact halo objects are expected to contribute, for given MACHO mass and halo fraction, for about one third of the overall MACHO signal (33)). To do so, however, a rather large number of events is necessary, and indeed the MEGA collaboration studied this statistics (39). Further care in this analysis is however suggested by the results by An et al. (87) who have shown that differential extinction in M31 might induce a similar asymmetric signal on the spatial distribution of self-lensing events. The distance from the M31 centre can be taken, in any case, as a useful zeroth order approximation (34; 51) as self-lensing events are expected to be more clustered around the M31 centre. A fourth available statistics is the flux deviation at maximum. However, this is only useful as a consistency check for the analysis, but it contains no information about the nature of the lenses.

The *number* of the expected events, in the central M31 region, from self lensing and MACHO lensing are about of the same order. The exact number depends on the M31 model, the field of view and the observational set up (besides the MACHO mass and halo fraction). We can take as an example the results reported in the analysis of Riffeser et al. (33) in their Table 2, for the expected signal in a field of view of about $17' \times 17'$ around the M31 centre. To be more specific, let consider compact halo objects of 0.5 $M_\odot$ and an halo mass fraction $f = 20\%$, about the preferred values from the MACHO LMC analysis (4). It then turns out that the number of expected self-lensing events is indeed larger, by about a factor of 1.5, than that of MACHO lensing ones[7].

This result can also be deduced by the top panels of Fig. 1 where we report the microlensing rate for bulge sources and bulge and M31 0.5 $M_\odot$ compact halo objects lenses (using the same models of (33)). Here the rate is evaluated per source star and for a fixed threshold impact parameter, $u_T = 1$, so that it can not be directly compared to the observations. However it clearly shows, first, the already stated asymmetry expected for M31 halo lensing events. Second, that self lensing, at least in the central region, is expected to give rise to a similar signal, as for the number of events, than MACHO lensing (note in particular the position of the line of equal rate at 10^{-5} events yr^{-1}).

To evaluate the actual number of expected events this expression of the rate must be multiplied, roughly the same overall factor for the different lens populations, for the number of available sources using the appropriate value for the threshold impact parameter, u_T. Depending on the luminosity function, the number of available sources follows the M31 surface brightness profile and peaks at the M31 centre. This explains the increase towards the M31 centre of the expected number of events for all the lens populations. On the other

[7]This outcome marks a relevant difference with respect to the LMC analyses where, even when considering the central bar region only, the number of expected MACHO lensing events outcomes that of self lensing (even if the exact contribution of LMC self lensing is still a debated issue (88; 89; 90; 91; 92)).

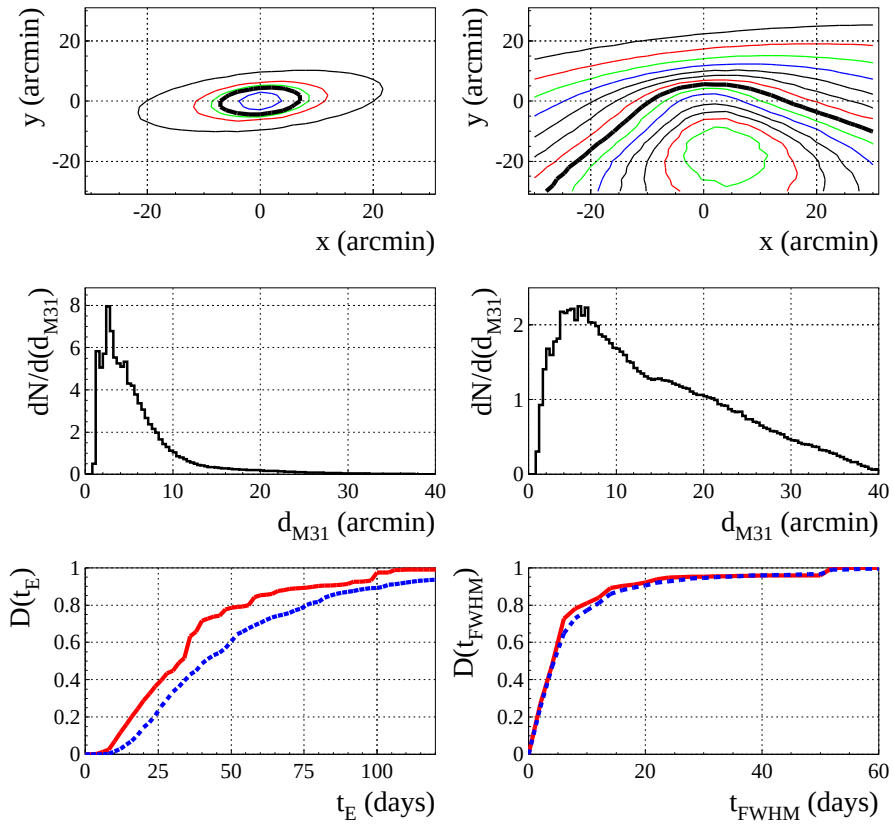

Fig. 1 The expected signal. Top panels: Microlensing rate per year per source star with $u_{\rm T} = {\rm cost} = 1$, for bulge sources and bulge (left) and M31 MACHO of 0.5 $M_\odot$ lenses. The $x-y$ axes are given in an intrinsic M31 coordinate system. The M31 models are as in (33). The contour levels are $0.1, 0.4, 0.7, 1.0, 2.5$ (left panel) and from 0.3 to 1.6 with $\Delta = 0.1$ with the thicker line marking the 1.0 level (always in units of 10^{-5} events yr^{-1}). Middle panels: Distance from the M31 centre distribution for self-lensing (left) and MACHO lensing. These distributions, with arbitrary normalization, are taken as an output of the Monte Carlo simulation of the POINT-AGAPE group presented in (34). Bottom panels: Cumulative distributions for $t_{\rm E}$ (left) and $t_{\rm FWHM}$ for bulge-bulge (solid lines) and M31 MACHO of 0.5 $M_\odot$. These distributions are taken as an output of the Monte Carlo simulation presented in (35).

hand, the threshold value for the impact parameter, $u_{\rm T}$, is a function of the line of sight (§ 2). Corresponding to the increase in the noise level following the M31 surface brightness, the threshold impact parameter decreases. As a final outcome, the expected number of lensing events, for both MACHO lensing and self lensing, moving towards the M31 centre first increases and then decreases with a turn off point determined by the specific observational set up. In Fig. 1, middle panels, we show the results of the Monte Carlo simulation for the POINT-AGAPE experiment, (34), for the distribution of

the expected distance from the M31 centre. Finally, moving towards the M31 centre, one must also face the problem of the increasing crowding of the field which further decreases the expected signal. To properly evaluate the extent of this effect is one of the main purposes of the detection efficiency analyses.

This result motivates the need of looking for microlensing events also in the outer regions of M31, where the expected self-lensing signal may be considered negligible. On the other hand, this is also where the expected overall rate becomes quite small, not a secondary issue as a main problem for the interpretation of the current experiments is the overall low rate of observed events. The analysis of the inner M31 region remains however essential, as the observation (or not) of the expected self-lensing signal may be used as a ruler for a given experiment.

The further relevant statistics we have from the observations is the event duration. As discussed in § 2, the directly accessible quantity is the full-width-half-maximum duration, $t_{\rm FWHM} = t_{\rm E} \cdot w(u_0)$. Once again, the threshold impact parameter, and its dependence on the background noise level, enters into play. In particular, at least for MACHO mass in the same range of stellar masses, the differences that exist in the physical duration distributions for MACHO lensing and self-lensing are almost completely washed out. It also turns out that, whatever the lens population, most of the events are expected to last a few days only. In Fig. 1, bottom panels, we show the cumulative distribution for the Einstein time and the full-width-halo-maximum timescales for the bulge sources and bulge and 0.5 $M_\odot$ M31 MACHO lenses configurations from the Monte Carlo simulation of the Loiano experiment discussed by the PLAN collaboration (35).

At a more refined level of analysis, a possible expected deviation from the standard Paczyński light curve that can be exploited for a deeper understanding of the lens nature is the finite size of the sources (93). Indeed, this effect can become relevant as most sources are expected to be bright giant stars, and in particular it has been shown to be suitable to distinguish MACHO lensing from self-lensing events (94). Furthermore, deviations from the point-like source light curve shape may also be used to constrain the lens proper motion (95). In turn, this is relevant as it may allow one to distinguish M31 lenses from Milky Way ones (96; 44).

3.5 Observational results

3.5.1 The microlensing candidate events

Microlensing events are distinguished from intrinsic variable signals for the *shape*, the *achromaticity* and the *unicity*. As for the shape, most of the events are expected, and found, to follow the symmetric bell-like Paczyński light curve. Any deviation (finite source effect, parallax, binary lens/source, ...), on the other hand, if explained in a microlensing context, can only reinforce the microlensing interpretation. On the other hand, because the background level

Table 2 Candidate microlensing events reported towards M31, as shown in Fig. 2. Seventh column: '$*$' indicates that the colour is $V-R$, '$**$' indicates that the colour is $B-R$.

id	RA (deg)	DEC (deg)	$d_{\rm M31}$ (arcmin)	$t_{\rm FWHM}$ (days)	$\Delta R_{\rm MAX}$	$R-I$	name	REF
1	10.672917	41.277528	0.72	5.3	17.9	0.8(**)	AGAPE-Z1	(40)
2	10.713333	41.398972	7.89	1.8	20.8	1.2(*)	PA-N1/MEGA-ML16	(44; 39)
3	11.087083	41.479111	22.07	22.0	19.1	1.0(*)	PA-N2/MEGA-ML7	(45; 38)
4	10.626250	41.216833	4.10	2.3	18.8	0.6	PA-S3/GL1	(45; 48; 46)
5	10.625000	40.896139	22.55	2.0	20.7	0.0	PA-S4/MEGA-ML11	(49; 38; 46)
6	10.552083	41.358333	8.01	16.0	21.0	2.2	C3	(42)
7	10.606667	41.440833	10.87	13.0	21.3	1.1	C4	(42)
8	10.470000	41.288333	9.74	14.0	21.8	0.5	C5	(42)
9	10.636667	41.332361	4.36	5.4	-	1.1	GL2	(48)
10	10.845417	41.091667	12.90	26.5	22.2	-	97-1267	(37)
11	10.762083	41.120694	9.58	17.3	20.3	-	97-3230	(37)
12	10.988750	41.198972	14.36	2.2	21.8	-	99-3688	(37)
13	10.793750	41.296611	5.19	5.4	21.8	0.6	MEGA-ML1	(38)
14	10.799583	41.295444	5.42	4.2	21.5	0.3	MEGA-ML2	(38)
15	10.815833	41.347833	7.56	2.3	21.6	0.4	MEGA-ML3	(38)
16	10.852083	41.630667	22.95	27.5	22.3	0.6	MEGA-ML8	(38)
17	11.195000	41.685194	33.90	2.3	22.0	0.2	MEGA-ML9	(38)
18	10.978750	41.175917	14.41	44.7	22.2	1.1	MEGA-ML10	(38)
19	10.760417	40.752556	31.19	26.8	23.3	0.8	MEGA-ML13	(38)
20	10.927083	40.709417	35.34	25.4	22.5	0.4	MEGA-ML14	(38)
21	10.509583	40.909722	22.98	3.4	19.5	-0.1	(PA-S16)	(46)
22	10.544583	41.329278	7.27	1.8	20.8	0.5	PA-N6	(34)
23	10.677500	41.211889	3.46	4.1	20.8	0.8(*)	PA-S7	(34)
24	10.888750	41.128889	12.49	59.0	20.1	1.3	NMS-E1	(43)
25	10.788750	41.348167	6.67	16.1	21.6	0.5	MEGA-ML15	(39)
26	10.481667	40.938889	21.85	10.1	22.2	0.4	MEGA-ML17	(39)
27	10.822083	41.037139	15.25	33.4	22.7	0.5	MEGA-ML18	(39)
28	10.737500	41.380556	7.09	7.1	21.1	1.0	OAB-N1	(35)
29	10.708333	41.311111	2.73	2.6	19.1	1.1	OAB-N2	(35)

has not, in general, the same colour than the lensed star, only the luminosity increase during the microlensing event is expected to be achromatic (26).

The very first concern of microlensing campaigns towards M31, in a regime where one can not resolve the source stars, was that of being able to detect microlensing events at all. After more than 10 years now of observational efforts, there are no doubts that microlensing events towards M31 have been observed.

The first microlensing candidate events reported towards M31 have been those presented by the VATT/Columbia collaboration (36). Although this represented a relevant result, as this clearly showed, for the first time, the possibility of such a detection, these flux variations (all of them of quite long duration and in fact lacking both a suitable sampling and a long enough baseline to robustly probe their unicity) have not been further discussed in the following works of the same collaboration, in particular in (37), so we are not going to consider them any longer.

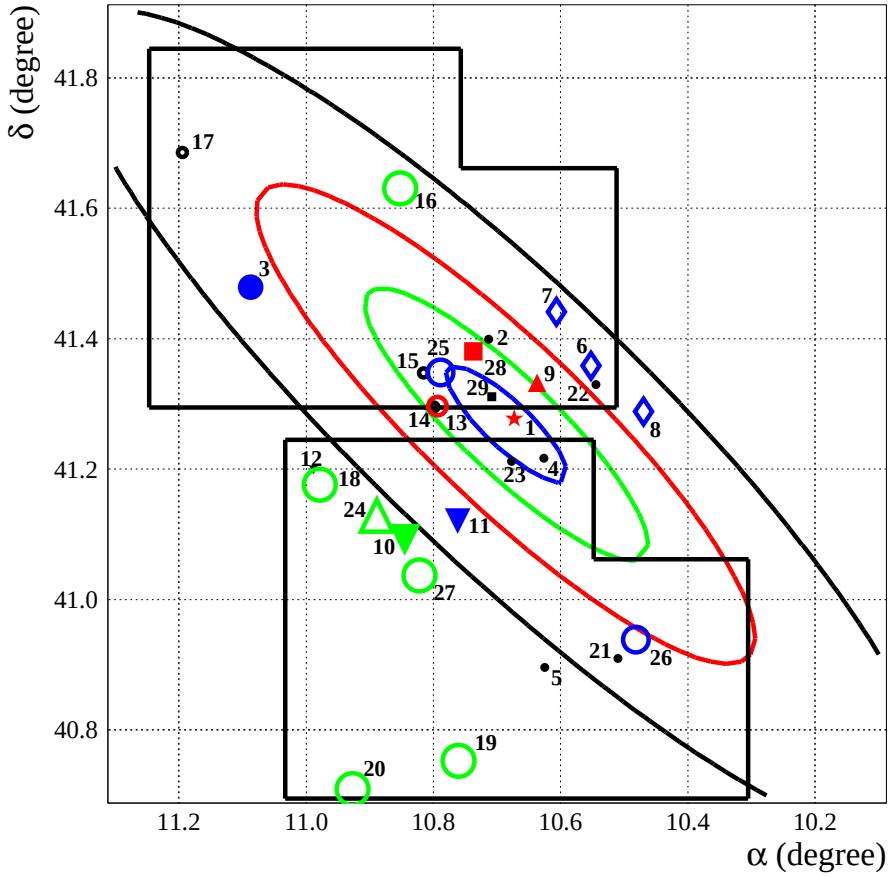

Fig. 2 Superimposed on iso-density contours of the M31 disc we report the position of the candidate microlensing events observed towards M31, indicated according to the numeration given in Table 2. The symbols refer to the collaboration that first reported an event: AGAPE (star), POINT-AGAPE (filled circles), SLOTT-AGAPE (empty diamonds), MEGA (empty circles), WeCAPP (filled upward triangle), VATT/Columbia (filled downward triangles), PLAN (filled boxes), NAINITAL (empty upward triangle). The size of the symbols is related to the event duration. Four bins are considered ($t_{\rm FWHM} < 5$ days, $5 < t_{\rm FWHM} < 10$ days, $10 < t_{\rm FWHM} < 25$ days and $t_{\rm FWHM} > 25$ days), with smaller symbols for shorter duration events (in the colour version, black, red, blue and green, respectively). Also reported, the contours of the two fields of view of the 2.5m INT campaign.

The first convincing microlensing candidate event towards M31, AGAPE-Z1, was then observed and characterised by the AGAPE collaboration (40). Indeed, its position and its shape, in particular its short duration, make of it a quite robust candidate. However, and this reason prevented at that time a sharper conclusion about its microlensing nature, although the possible intrinsic variable contaminations were carefully analysed and ruled out, the lack

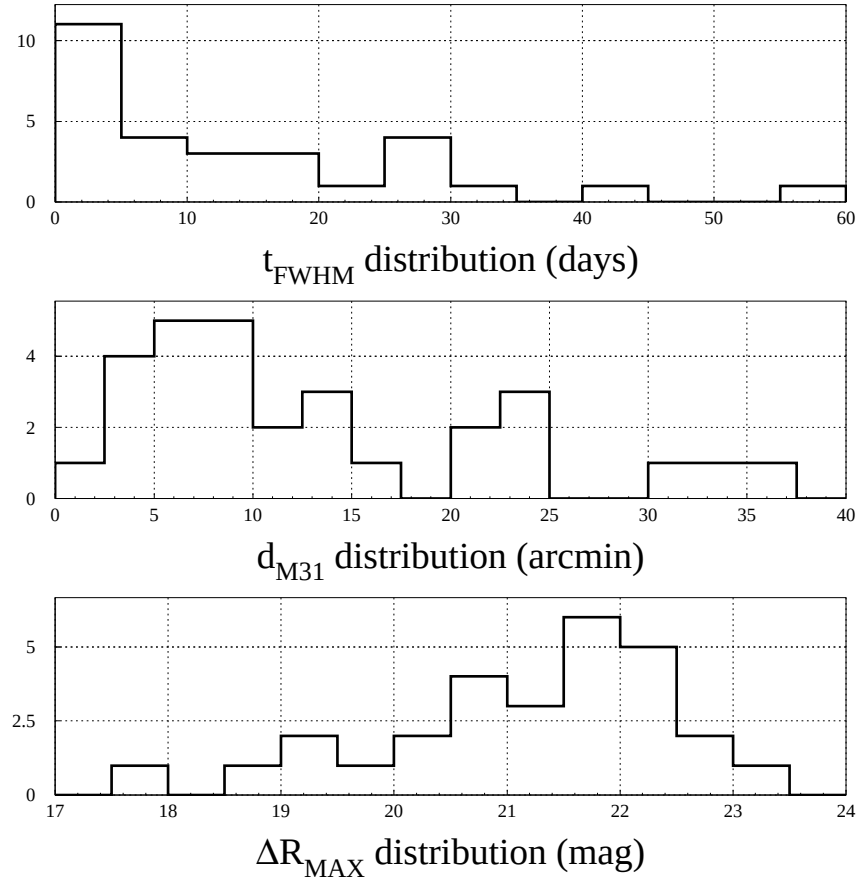

Fig. 3 For the candidate microlensing events observed towards M31, Table 2, we report, from top to bottom, the distribution of the duration, $t_{\rm FWHM}$, of the distance from the M31 centre, $d_{\rm M31}$ and of the flux deviation at maximum expressed in term of magnitude, $\Delta R_{\rm MAX}$.

of a suitable coverage of the flux deviation in two colours did not allow the achromaticity to be properly tested.

In Table 2 we report all the microlensing candidate events that have been reported up to now. A few of them have been detected independently by more than one collaboration (this holds in particular for the POINT-AGAPE and the MEGA group who shared the same set of INT data). The total number of events sums up to 29.

In particular, from the analysis of Belokurov et al. (46) we report only the three "first level" candidates. The only new one with respect to the previous POINT-AGAPE analyses was PA-S16 (this is a POINT-AGAPE internal name only, in that paper it was simply indicated as "candidate 1"). Three "second

level" candidates were also reported, all of them quite faint and of rather long duration, $t_{\rm FWHM} > 30$ days, and 16 "third level" ones. Noteworthy, 11 out of these 16 lie at more than 12' from the M31 centre.

Most of the sources of M31 microlensing events are expected to be bright giants stars (26), that should be visible, therefore, on HST images. Indeed, an identification of the source has been reported for a few events. This is extremely important in particular as it allows one to break the parameter degeneracy and to measure the physical timescale $t_{\rm E}$.

In Fig. 2 we report, superimposed on the isodensity contours of the M31 disk, the position of these candidate events.

In Fig. 3 we report, for this set of observed candidate events, the distribution of the duration $t_{\rm FWHM}$, the flux deviation at maximum, expressed in term of magnitude, $\Delta R_{\rm MAX}$, and of the distance from the M31 centre. Looking at these distributions, we note that most of the reported events have a quite short duration, $t_{\rm FWHM} < 10$ days, and are clustered around the inner M31 region. These outcomes match well the theoretical expectations (§ 3.4) and are relevant with respect to the issue of the possible contamination of variable stars to the microlensing signal.

Because of their intrinsically non-repeating nature, most of the time it is difficult to completely rule out the possibility of an intrinsic variable contamination and altogether drop the qualification of *candidate* for a reported microlensing event. For single events this is actually possible if the light curve shape deviates, in a microlensing-like way, from the smooth Paczyński shape, for instance for binary events. This might be the case for at least one of the M31 pixel-lensing events, PA-N2. On the other hand, for a large enough set of events this is possible statistically if the observed signal characteristics match the expected ones.

The background noise to the microlensing signal is given by intrinsically variable stars. In the pixel-lensing regime many stars contribute to the flux of each pixel. Even if not bright enough to give rise to a detectable signal over the background noise level, these can add an additional, non-gaussian, noise to the light curve (with the extreme case being, as for PA-N1, of a bonafide microlensing event superimposed on the same light curve of a variable star). This is indeed a relevant issue as for our ability to select microlensing events at all (so that it concerns the *efficiency* of a selection pipeline). Second, there might be variable stars masquerading as microlensing events, and this indeed is the biggest single problem in the interpretation of microlensing events. For a typical pixel-lensing campaign one monitors thousands of flux variations due to intrinsic variable stars to be compared with a few (if any) microlensing signals. Variable stars contaminating the microlensing signal should reside either in our Galaxy or in M31 itself, or might be background supernovæ. For (unique flux variation) candidate events of short duration and located near to the M31 centre, all of these possible form of contamination can be, even if not absolutely ruled out, safely excluded (34). (For instance, a few flux variations first claimed to be microlensing candidates, located in the inner M31 region but with a quite large timescale (41), have been in a second moment, once the analysis extended

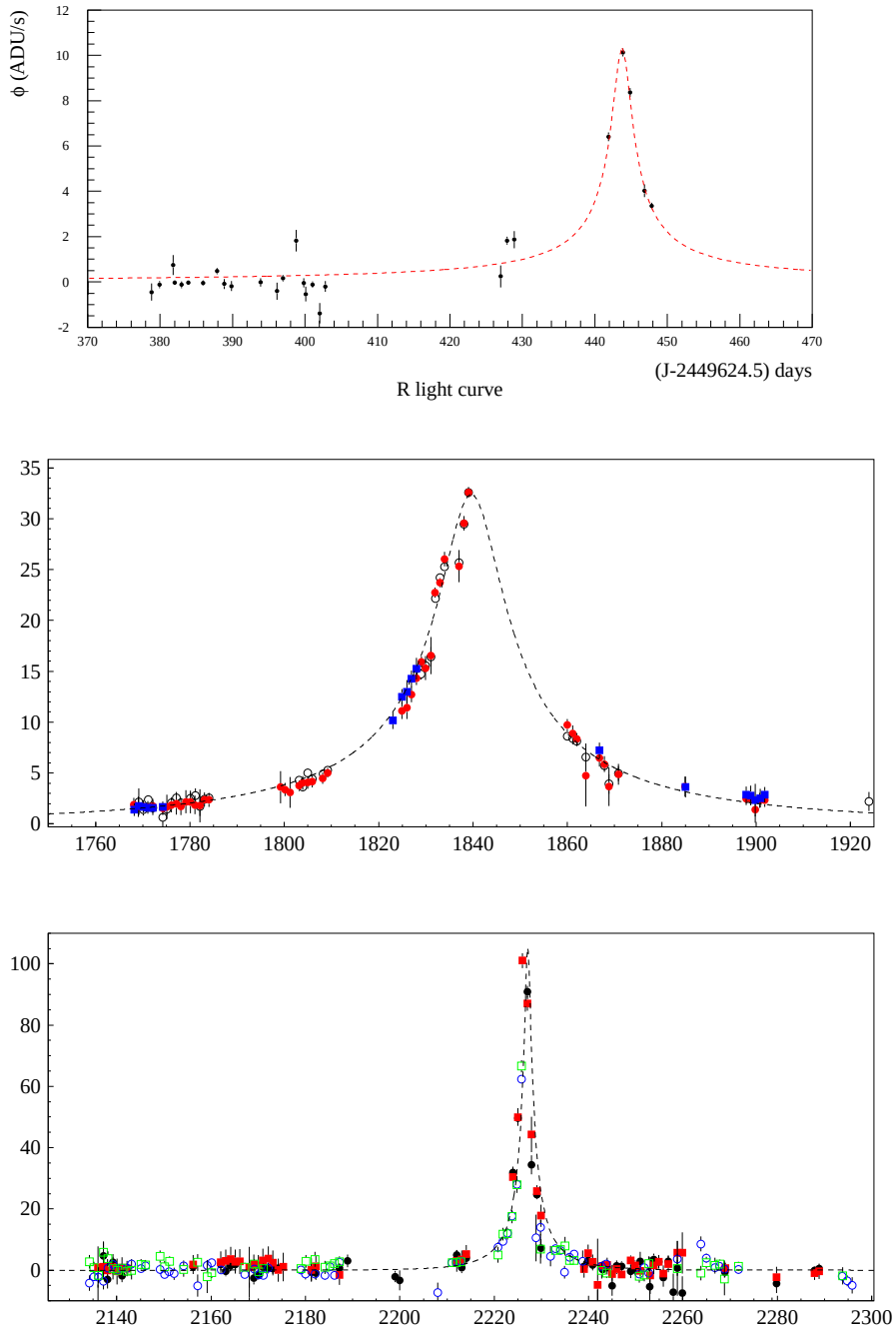

Fig. 4 The light curves for three pixel lensing (candidate) events observed towards M31. From top to bottom: AGAPE-Z1 (Figure reproduced from Fig. 3 of (40)); POINT-AGAPE PA-N2/MEGA ML7 (Figure adapted from (45)); POINT-AGAPE S3/WeCAPP GL1 (Figure adapted from (45; 48)). The dashed curves represent the best Paczyński light curve fits. The units on the axes (middle and bottom panels) are the same as in the top panel. Middle panel: empty/filled circles and filled boxes are for g', r' and i' band data respectively (black, red and blue in the colour version). Bottom panel: circles and boxes are for R and I band data, filled and empty symbols for the POINT-AGAPE and WeCAPP data sets.

over a longer baseline, probed to be due to intrinsically variable stars (42).) While this argument can be used statistically for large enough set of events, for single events, for which a long enough flat baseline (a usual demand in any selection pipeline) can be taken as a strong proof against the contamination of repeating variables, the single one more dangerous form of contamination comes from eruptive variables. This possibility must be carefully considered case by case, with particular attention to the *shape* and the *colour* of the candidate event.

Looking back at the distributions shown in Fig. 3 we may indeed wonder whether long duration and faint events, the most easily to be confused with underlying background variable stars, can be looked at as outliers of a truly microlensing distribution.

Besides AGAPE-Z1 (Fig. 4, top panel), a few more events deserve some more comments. PA-N1 (44) is characteristic in that its light curve is clearly contaminated by a nearby variable. Its short duration, good sampling and probed achromaticity make of it a robust microlensing event. Furthermore, the possible source has been identified on some HST frame (this identification, however, has been challenged by Cseresnjes et al. (97)). PA-N2 (45)/MEGA-ML7 (38), Fig. 4 middle panel, is in many ways a peculiar nonetheless extremely robust microlensing event. This is because of its long duration, very large brightness at maximum amplification and location, far away from the M31 centre. In fact, this variation has been observed and well sampled, for most of its (long) bump, in three colours, so that the expected achromaticity has been extremely well verified. It is going to be interesting, once the statistics of observed events will enlarge with new observational campaigns, to see whether other events with similar characteristics will be observed or not. Furthermore, the PA-N2 light curve shows a deviation from the simple Paczyński shape. This anomaly has been the object of a thorough analysis of the POINT-AGAPE collaboration. In particular, An et al. (98) probed it to be compatible with a binary lens system. Because of all of these reasons PA-N2 looks as a robust microlensing event on its own right. PA-S3 (45)/GL1 (48), besides being, as expected for the "typical" M31 pixel-lensing events, short and near the M31 centre, has been observed both in the INT and the WeCAPP data set. The joined light curve gives an extremely convincing bonafide microlensing event (Fig. 4, bottom panel). We also recall PA-S4 (49)/MEGA-ML11(38), located roughly along the line of sight of M32, a companion galaxy of M31, which is a convincing inter-galactic microlensing event (49). Finally we mention PA-S5 (34): although this flux variation has *not* been selected by the microlensing selection pipeline (so that it even lacks the status of *candidate* event), still, it looks extremely interesting. Its shape, not to be easily explained by any intrinsic variable, deviates significantly from the Paczyński one in a way that is suggestive of a possible binary lens configuration. However, the poor sampling along the bump did not allow its full characterization. A further reason of interest is its position, about $20'$ away from the M31 centre.

3.5.2 Looking for compact halo objects (and self-lensing events)

Once acknowledged the possibility to detect and characterize microlensing events in the pixel-lensing regime towards M31, the leading scientific question that has been addressed is the search for dark matter in form of compact halo objects. As already outlined, a main problem is the ability to distinguish MACHO lensing events from self-lensing ones. In fact, as we detail below, the main results reported up to now are in disagreement on the MACHO halo content, and this can be traced back mainly to this issue.

The first attempt to draw conclusions on the MACHO content towards M31 has been carried out by Uglesich et al. (37), who concluded for an evidence of a MACHO signal. The next analyses, from the POINT-AGAPE and the MEGA collaboration, presented their results with more detailed and reliable efficiency analyses, an essential step to meaningfully compare the observed and the expected signal.

POINT-AGAPE and MEGA made use of the same INT data set (although MEGA considered a fourth year of data not included in the POINT-AGAPE analysis).

POINT-AGAPE reported an *evidence* for a MACHO signal towards M31 (34). In particular they have evaluated a *lower* limit for the halo fraction in form of MACHOs, f, of about 20% in the mass range $0.1 - 1$ $M_\odot$. On the other hand, MEGA concluded (39) that their observed rate was consistent with the expected self-lensing signal. In particular they ruled out a MACHO halo fraction, for 0.5 $M_\odot$ compact halo objects, larger than 30%.

POINT-AGAPE restricted the search of microlensing events to short duration, $t_{\rm FWHM} < 25$ days, and bright, $\Delta R_{\rm MAX} < 21$, flux variations. With a thorough discussion to exclude the contamination of intrinsic variable objects they presented 5 microlensing candidate events upon which they based their following analysis[8]. Without any a priori cut in the event parameter space, MEGA presented 14 microlensing candidate events. All the additional events with respect to POINT-AGAPE can be explained because of the enlarged parameter space and the extended overall baseline. Besides, MEGA failed to report the detection of 2 of the POINT-AGAPE candidates (plus a third one detected nearby the M31 centre in a region MEGA excluded from his analysis).

To evaluate the expected signal, POINT-AGAPE developed a full Monte Carlo simulation completed by an efficiency analysis where the events selected within the Monte Carlo were injected in the data and submitted to the analysis pipeline. MEGA evaluated the microlensing rate taking into account the pipeline detection efficiency. As a result, for their fiducial model, to be specific we are going hereafter to consider MACHOs of 0.5 $M_\odot$ and fix $f = 20\%$, POINT-AGAPE reported an expected self-lensing signal of about 0.8 events to be compared with 1.4 MACHO events, MEGA of 14 versus 6.2 events, respectively. Besides the overall numbers, that can not be directly compared

[8] A sixth candidate events, PA-S4, was not included as acknowledged to be, more likely, an intergalactic M31-M32 event.

because of the different regions in the event parameter space explored, a striking difference is in the expected *ratio* of self-lensing over MACHO lensing.

In order to evaluate the probability function for f, POINT-AGAPE have taken a specific care in order to include the information on the spatial distribution of the observed events. In fact, the position of PA-N2 , § 3.5.1, well away from the M31 inner region where self lensing is expected to be relatively small with respect to the would be MACHO signal, turned out to be essential to conclude on the "evidence" for the MACHO signal. On the other hand, a main weakness in the POINT-AGAPE analysis is the small statistics. This holds in particular because the reported result heavily depends on a single, though extremely robust by itself, microlensing candidate (PA-N2). Furthermore, MEGA argued that the M31 model used by POINT-AGAPE was bound to unduly *underestimate* the expected self-lensing signal even though POINT-AGAPE claimed to have paid attention, for his fiducial model, to actually consider *stellar* lenses only to account for self lensing. Besides, POINT-AGAPE have tested their results also for more massive luminous models, § 3.3, always finding evidence for a MACHO signal.

Although the analysis on the *number* of observed candidates versus expected self-lensing events clearly points towards the self-lensing explanation of the observed rate, a weakness in the MEGA analysis can be found in that they seem to underestimate the role played by the characteristics of the observed events. In particular, the spatial distribution of the events, both for a signal of asymmetry and because quite a large fraction of them lie far from the innermost M31 region, seems indeed, as in fact also pointed out by MEGA (see in particular their Fig. 18), to favour MACHO lensing over self lensing. (Besides, in their previous analysis, de Jong et al. (38), the MEGA collaboration had preliminarly concluded that "the spatial distribution of candidate microlenses is suggestive of the presence of a microlensing halo", and more specifically "dark" halo). The spatial distribution, and a few more issues, have been also analysed by Ingrosso et al. (99; 100) who concluded that self lensing can hardly explain all of the MEGA microlensing candidates.

These analyses clearly have left the MACHO issue, as for the line of sight towards M31, still open. They also show the extent to which a correct modelling of M31, in particular of its luminous components, is extremely relevant. In fact, this should be taken as an opportunity of the need of a better astrophysical understanding both of the expected signal and of the observed events.

Along this direction the WeCAPP collaboration made a relevant contribution with an extremely detailed analysis of the PA-S3/GL1 event (94). The joint analysis of INT and WeCAPP data allowed them to strongly constrain this event. Furthermore, a specific analysis on the relevance of the finite source effect, considering in particular the extremely large brightness of the event, and carefully including an analysis of all the event characteristics, allowed the authors to conclude on the much more likely MACHO, rather than stellar, nature of the lens. It is also noteworthy that this result is reached although, § 3.5.1, this event lies at very short distance from the M31 centre, where self-lensing

signal is expected to be quite large with respect to MACHO lensing. Finally, it is worth stressing the methodological importance of such a joint analysis of different data sets (even reduced following different photometry schemes) that in particular allowed to robustly confirm the microlensing nature of this flux variation. This is a quite obvious outcome for Galactic bulge searches and it clearly suggests the way to be followed also for M31 analyses.

3.6 The hunt for extra-solar (extra-galactic) planets

Beyond the search for MACHOs microlensing is, together with other techniques (see e.g. the review in (101)), a suitable tool for the detection of extra-solar planets (102; 103). The microlensing signal for a planetary system is that of a binary lens with extremely small mass ratio, q, and it shows itself as a short duration perturbation of the smooth single lens light curve. Only of order of ten planets have been detected, towards the Galactic bulge, using microlensing (e.g. (104)) against a few hundreds with other methods (mainly, radial velocity and transit). However, microlensing has various advantages over other methods (105; 106). In particular, microlensing is the only available tool sensitive to extra-solar planets at large distance from the solar system, up to extra-galactic distances.

Covone et al. (107) and Baltz & Gondolo (108) have been the first to discuss the possibility to detect extra-solar planets in M31 with pixel lensing. More recently, Chung et al. (109), addressed this issue within the specific experimental set up of the ANGSTROM project discussing, in particular, the efficiency for detecting planets of Jupiter-mass within the lensing zone using a full network of telescopes. Ingrosso et al. (110) have analysed the same issue with the additional bonus of using a Monte Carlo approach spanning both the parameter space of the lens-planet system as well as that of the underlying lensing events. In particular, they have pointed out that a $\sim$ 6-Jupiter mass planet in M31 might already have been detected. In fact, the anomaly of the POINT-AGAPE PA-N2 candidate event had already been discussed to be compatible with a binary lens system with an extremely small mass ratio (98). As a caveat for this exciting outcome we recall the extremely large uncertainties in the lens mass determination (and therefore on that of its companion). Whatever be the case with PA-N2, from the above considerations it clearly appears that the detection of planets in M31 is already a reachable objective. To this purpose, however, a similar strategy, with the caveats suggested by all the peculiarities of the pixel-lensing regime, as that followed for microlensing planet searches towards the Galactic bulge, with survey and follow up all around the world, is needed.

Finally, we mention a relevant byproduct of M31 pixel lensing searches, as of all microlensing analyses, namely the study of variable stars. This is both interesting in itself but also as a way to better understand the microlensing signal. We have already mentioned a relevant outcome from the thorough analysis of the POINT-AGAPE catalogue (87). We also recall the specific analyses

of Novæ by POINT-AGAPE (111; 112), the AGAPE (113) and WeCAPP M31 variable star catalogues (114), and the Nainital analyses (115; 116).

4 Pixel lensing beyond the Local Group

The pixel lensing technique allows the search for (stellar) microlensing events to be extended beyond the limit of the Local Group. This opportunity is extremely challenging, also because, at such large distance, one fully enters the "spike" regime, § 2. Pixel lensing is only moving his first steps in this direction, nonetheless it already clearly probed to be a viable tool of analysis.

A first possible target was soon identified to be the giant elliptical galaxy M87 at the centre of the Virgo Cluster. In (117) Gould addressed this problem and made a detailed proposal for a WFPC2/HST campaign with this purpose. Baltz et al (118) carried out this ambitious programme with a campaign lasting 30 days. In particular, they reported the detection of seven variable sources among those they identified one viable microlensing candidate consistent with a dark matter halo mass fraction of about 20% of microlensing objects for both M87 and the Virgo cluster.

A few other targets have also been proposed: the cluster A2152 in (119) and A2218 and A370 in (120). More recently, de Jong et al. (121) carried out a microlensing pilot campaign looking at Centaurus A using the ESO/MPG 2.2m telescope, showing in particular the feasibility of the project.

5 Conclusion

Pixel lensing is stellar microlensing of unresolved sources (a situation characterized, as we have outlined, by the fact that the photon noise is dominated by that of the background level). It allows the realm of microlensing to be extended to distant targets, in the Local Group and beyond. In this review we have focused on the main observational results obtained up to now. The principal target for observations has been our nearby galaxy, M31.

Pixel lensing has probed to be able to confidently detect and robustly characterize microlensing events. The original microlensing motivation, the search for the (dark matter) compact halo objects (MACHOs) signal, is still an open issue. In the meantime it has become clear the importance of a correct understanding of self lensing, for which the lens belongs to some luminous population, both as a background signal to MACHO lensing and as an opportunity in itself for the study of the luminous lensing components.

The detection of about 30 microlensing candidate events has been reported towards M31. In particular, out of a complete analysis on the same INT data set, the POINT-AGAPE collaboration concluded for an evidence of a MACHO signal whereas the MEGA collaboration rather found its detected signal to be compatible with the expected self-lensing one. On the other hand, the careful analysis of an extremely well sampled event (with two different data sets)

allowed the WeCAPP collaboration to conclude on the more likely MACHO rather than stellar nature for the lens of a bright event detected in the central M31 region.

These results motivate to further carry on both the theoretical and the observational efforts. In fact, pixel lensing is now entering a new phase of maturity, rich in opportunities not to be missed, with in particular the need for a deeper understanding of the microlensing signal from an astrophysical point of view. The increase of the understanding of the lensing signal with the ongoing campaign (ANGSTROM and PLAN), the effort to establish a real time analysis to be used for a network of telescopes (ANGSTROM), as well as the significant increase also in the number of events expected with the PAandromeda project, with the perspective of an invaluable full coverage of M31, are the next to come and essential steps towards this purpose.

Beyond the search for dark matter in form of compact halo objects, and more generally the study of the luminous M31 lens populations with self lensing, M31 pixel lensing is beginning to face also a new challenging purpose, still already within the reach of the present technology, the search for extra-solar, extra-galactic, planets. This is an additional (if needed) strong motivation for M31 pixel lensing searches.

Note added in proof

The WeCAPP collaboration (A. Riffeser and S. Seitz, private communication) is currently completing the final analysis of their 11-years campaign (Riffeser et al., 2010, in preparation and Koppenhöfer et al., 2010, in preparation). They report the detection of 10 microlensing events (all of them with very short duration and specifically, 8 out of 10 with $t_{\rm FWHM} < 5$ days). Their preliminar results on the expected rate indicate that the self-lensing signal alone is not sufficient to explain all of the observed events.

Acknowledgements It is a pleasure to thank the editors of the present volume, and in particular Ph. Jetzer, for giving me the opportunity to write this review. I would like to thank the AGAPE group, in particular Y. Giraud-Hèraud, J. Kaplan, M. Crézé and P. Baillon, for introducing and carrying me on through this fascinating subject in the course of several years. I acknowledge support for this work by the Italian Space Agency (ASI) and by the "Istituto Internazionale per gli Alti Studi Scientifici" (IIASS).

References

1. B. Paczyński, ApJ, **304**, 1 (1986)
2. M. Moniez, Microlensing towards the galactic center and LMC/SMC, This volume
3. M. Dominik, Microlensing and planet detection, This volume
4. C. Alcock, R.A. Allsman, D.R. Alves, et al., ApJ, **542**, 281 (2000)
5. D.P. Bennett, ApJ **633**, 906 (2005)
6. P. Tisserand, L. Le Guillou, C. Afonso, et al. A&A, **469**, 387 (2007)

7. L. Wyrzykowski, S. Kozlowski, J. Skowron, et al. MNRAS, **397**, 1228 (2009)
8. J. Wambsganss, Extragalctic microlensing, This volume
9. B. Paczynski, ARA&A, **34**, 419 (1996)
10. E. Roulet, S. Mollerach, Phys. Rep., **279**, 67 (1997)
11. J. Wambsganss, *Gravitational Microlensing* in Gravitational Lensing: Strong, Weak and Micro, Saas-Fee Advanced Courses, Volume 33. Springer-Verlag Berlin Heidelberg, p. 453 (2006)
12. A. Gould, ApJ, **470**, 201 (1996)
13. P. Popowski, K. Griest, C.L. Thomas, et al. ApJ, **631**, 879 (2005)
14. C. Hamadache, L. Le Guillou, P. Tisserand, et al. A&A, **454**, 185 (2006)
15. T. Sumi, P.R. Woźniak, A. Udalski, et al., ApJ, **636**, 240 (2006)
16. P. Wozniak, B. Paczynski, ApJ, **487**, 55 (1997)
17. P. Gondolo, ApJ, **510**, L29 (1999)
18. E.A. Baltz, J. Silk, ApJ, **530**, 578 (2000)
19. M. Dominik, MNRAS, **393**, 816 (2009)
20. E. Kerins, B.J. Carr, N.W. Evans, et al., MNRAS, **323**, 13 (2001)
21. A. Melchior, C. Afonso, R. Ansari, et al., A&A **339**, 658 (1998)
22. A. Melchior, C. Afonso, R. Ansari, et al., A&ASS **134**, 377 (1999)
23. A.P.S. Crotts, ApJ, **399**, L43 (1992).
24. P. Baillon, A. Bouquet, Y. Giraud-Heraud, J. Kaplan, A&A, **277**, 1 (1993)
25. A.B. Tomaney, A.P.S. Crotts, AJ, **112**, 2872 (1996)
26. R. Ansari, M. Aurière, P. Baillon, et al., A&A, **324**, 843 (1997)
27. P. Jetzer, A&A, **286**, 426 (1994)
28. W.N. Colley, AJ, **109**, 440 (1995)
29. C. Han, ApJ, **472**, 108 (1996)
30. G. Gyuk, A. Crotts, ApJ, **535**, 621 (2000)
31. E.A. Baltz, G. Gyuk, A. Crotts, ApJ, **582**, 30 (2003)
32. E.A. Baltz, ApJ, **624**, 168 (2005)
33. A. Riffeser, J. Fliri, S. Seitz, R. Bender, ApJSS **163**, 225 (2006)
34. S. Calchi Novati, S. Paulin-Henriksson, J. An, et al., A&A, **443**, 911 (2005)
35. S. Calchi Novati, V. Bozza, F. DePaolis, et al., ApJ, **695**, 442 (2009)
36. A.P.S. Crotts, A.B. Tomaney, ApJ, **473**, L87 (1996)
37. R.R. Uglesich, A.P.S. Crotts, E.A. Baltz et al., ApJ, **612**, 877 (2004)
38. J.T.A. de Jong, K. Kuijken, A.P.S. Crotts et al., A&A, **417**, 461 (2004)
39. J.T.A. de Jong, L.M. Widrow, P. Cseresnjes, et al., A&A, **446**, 855 (2006)
40. R. Ansari, M. Aurière, P. Baillon, et al., A&A, **344**, L49 (1999)
41. S. Calchi Novati, G. Iovane, A.A. Marino, et al., A&A, **381**, 848 (2002)
42. S. Calchi Novati, P. Jetzer, G. Scarpetta, et al., A&A, **405**, 851 (2003)
43. Y.C. Joshi, A.K. Pandey, D. Narasimha, R. Sagar, A&A, **433**, 787 (2005)
44. M. Aurière, P. Baillon, A. Bouquet, et al., ApJ, **553**, L137 (2001)
45. S. Paulin-Henriksson, P. Baillon, A. Bouquet, et al., A&A, **405**, 15 (2003)
46. V. Belokurov, J. An, N.W. Evans, et al., MNRAS, **357**, 17 (2005)
47. A. Riffeser, J. Fliri, C.A. Gössl, et al., A&A, **379**, 362 (2001)
48. A. Riffeser, J. Fliri, R. Bender, S. Seitz, C.A. Gössl, ApJ, **599**, L17 (2003)

49. S. Paulin-Henriksson, P. Baillon, A. Bouquet, et al., ApJ, **576**, L121 (2002)
50. E. Kerins, M.J. Darnley, J.P. Duke, et al., MNRAS, **365**, 1099 (2006)
51. S. Calchi Novati, G. Covone, F. de Paolis, et al., A&A, **469**, 115 (2007)
52. M.J. Darnley, E. Kerins, A. Newsam, et al., ApJ **661**, L45 (2007)
53. D. Kim, S.J. Chung, M.J. Darnley, et al., ApJ **666**, 236 (2007)
54. A.W. McConnachie, M.J. Irwin, A.M.N. Ferguson, et al., MNRAS **356**, 979 (2005)
55. G.A. Tammann, A. Sandage, B. Reindl, ApJ **679**, 52 (2008)
56. R.A.M. Walterbos, R.C. Kennicutt, Jr., A&ASS **69**, 311 (1987)
57. S.M. Kent, AJ **97**, 1614 (1989)
58. L. Chemin, C. Carignan, T. Foster, ApJ in press, arXiv:0909.3846
59. J.J. Geehan, M.A. Fardal, A. Babul, P. Guhathakurta, MNRAS **366**, 996 (2006)
60. L.M. Widrow, K.M. Perrett, S.H. Suyu, ApJ **588**, 311 (2003)
61. E. Tempel, A. Tamm, P. Tenjes, arXiv:0707.4374
62. A. Klypin, H. Zhao, R.S. Somerville, ApJ **573**, 597 (2002)
63. M. Montalto, S. Seitz, A. Riffeser, et al., arXiv:0907.0669
64. S.M. Kent, ApJ **266**, 562 (1983)
65. S.M. Kent, AJ **91**, 1301 (1986)
66. S.M. Kent, AJ **94**, 306 (1987)
67. L.M. Widrow, J. Dubinski, ApJ **631**, 838 (2005)
68. E. Athanassoula, R.L. Beaton, MNRAS **370**, 1499 (2006)
69. R.L. Beaton, S.R. Majewski, P. Guhathakurta, et al., ApJ **658**, L91 (2007)
70. R.P. Saglia, M. Fabricius, R. Bender, et al. A&A in press, arXiv:0910.5590
71. A.S. Font, K.V. Johnston, A.M.N. Ferguson, et al., ApJ **673**, 215 (2008)
72. M. Tanaka, M. Chiba, Y. Komiyama, P. Guhathakurta, J.S. Kalirai, M. Iye, arXiv:0908.0245
73. A.M.N. Ferguson, M.J. Irwin, R.A. Ibata, G.F. Lewis, N.R. Tanvir, AJ **124**, 1452 (2002)
74. J.C. Richardson, A.M.N. Ferguson, R.A. Johnson, et al., AJ **135**, 1998 (2008)
75. R.M. Rich, K.J. Mighell, ApJ **439**, 145 (1995)
76. A.W. Stephens, J.A. Frogel, D.L. DePoy, et al., AJ **125**, 2473 (2003)
77. A. Sarajedini, P. Jablonka, AJ **130**, 1627 (2005)
78. K.A.G. Olsen, R.D. Blum, A.W. Stephens, T.J. Davidge, P. Massey, S.E. Strom, F. Rigaut, AJ **132**, 271 (2006)
79. J. Yin, J.L. Hou, N. Prantzos, S. Boissier, R.X. Chang, S.Y. Shen, B. Zhang, A&A **505**, 497 (2009)
80. S.K. Ballero, P. Kroupa, F. Matteucci, A&A **467**, 117 (2007)
81. R.P. van der Marel, P. Guhathakurta, ApJ **678**, 187 (2008)
82. R. Braun, ApJ **372**, 54 (1991)
83. J.F. Navarro, C.S. Frenk, S.D.M. White, ApJ **462**, 563 (1996)
84. J.F. Navarro, C.S. Frenk, S.D.M. White, ApJ **490**, 493 (1997)
85. D. Merritt, A.W. Graham, B. Moore, J. Diemand, B. Terzić, AJ **132**, 2685 (2006)

86. S. Calchi Novati, F. de Luca, P. Jetzer, L. Mancini, G. Scarpetta, A&A **480**, 723 (2008)
87. J.H. An, N.W. Evans, P. Hewett, et al., MNRAS **351**, 1071 (2004)
88. G. Gyuk, N. Dalal, K. Griest, ApJ **535**, 90 (2000)
89. P. Jetzer, L. Mancini, G. Scarpetta, A&A **393**, 129 (2002)
90. L. Mancini, S. Calchi Novati, P. Jetzer, G. Scarpetta, A&A **427**, 61 (2004)
91. S. Calchi Novati, F. De Luca, P. Jetzer, G. Scarpetta, A&A **459**, 407 (2006)
92. S. Calchi Novati, L. Mancini, G. Scarpetta, Ł. Wyrzykowski, MNRAS **400**, 1625 (2009)
93. H.J. Witt, S. Mao, ApJ **430**, 505 (1994)
94. A. Riffeser, S. Seitz, R. Bender, ApJ **684**, 1093 (2008)
95. A. Gould, ApJ **421**, L71 (1994)
96. C. Han, A. Gould, ApJ **473**, 230 (1996)
97. P. Cseresnjes, A.P.S. Crotts, J.T.A. de Jong, et al., ApJ, **633**, L105 (2005)
98. J.H. An, N.W. Evans, E. Kerins, et al. ApJ, **601**, 845 (2004)
99. G. Ingrosso, S. Calchi Novati, F. de Paolis, et al., A&A, **445**, 375 (2006)
100. G. Ingrosso, S. Calchi Novati, F. de Paolis, et al., A&A, **462**, 895 (2007)
101. M. Perryman, O. Hainaut, D. Dravins, et al., arXiv:astro-ph/0506163
102. S. Mao, B. Paczynski, ApJ **374**, L37 (1991)
103. A. Gould, A. Loeb, ApJ **396**, 104 (1992)
104. A. Gould, *ASPC*, vol. 403, ed. by K. Z. Stanek (2009), vol. 403, p. 86, arXiv:0803.4324
105. M. Dominik, U.G. Jorgensen, K. Horne, et al., arXiv:0808.0004
106. J.P. Beaulieu, E. Kerins, S. Mao, et al., arXiv:0808.0005
107. G. Covone, R. de Ritis, M. Dominik, A.A. Marino, A&A **357**, 816 (2000)
108. E.A. Baltz, P. Gondolo, ApJ **559**, 41 (2001)
109. S.J. Chung, D. Kim, M.J. Darnley, et al., ApJ **650**, 432 (2006)
110. G. Ingrosso, S. Calchi Novati, F. de Paolis, et al., MNRAS **399**, 219 (2009)
111. M.J. Darnley, M.F. Bode, E. Kerins, et al., MNRAS **353**, 571 (2004)
112. M.J. Darnley, M.F. Bode, E. Kerins, et al., MNRAS **369**, 257 (2006)
113. R. Ansari, M. Aurière, P. Baillon, et al., A&A **421**, 509 (2004)
114. J. Fliri, A. Riffeser, S. Seitz, R. Bender, A&A **445**, 423 (2006)
115. Y.C. Joshi, A.K. Pandey, D. Narasimha, R. Sagar, Y. Giraud-Héraud, A&A **402**, 113 (2003)
116. Y.C. Joshi, A.K. Pandey, D. Narasimha, Y. Giraud-Héraud, R. Sagar, J. Kaplan, A&A **415**, 471 (2004)
117. A. Gould, ApJ, **455**, 44 (1995)
118. E.A. Baltz, T.R. Lauer, D.R. Zurek, et al., ApJ, **610**, 691 (2004)
119. T. Totani, ApJ, **586**, 735 (2003)
120. A.V. Tuntsov, G.F. Lewis, R.A. Ibata, J. Kneib, MNRAS **353**, 853 (2004)
121. J.T.A. de Jong, K.H. Kuijken, P. Héraudeau, A&A, **478**, 755 (2008)
122. P. Baillon, A. Bouquet, Y. Giraud-Héraud, J. Kaplan, in *Particle Astrophysics*, ed. by G. Fontaine & J. Tran Thanh van (1993), pp. 529–+

123. Paul Baillon, Alain Bouquet, Yannick Giraud-Héraud, and Jean Kaplan, In Gérard Fontaine and Jean Trân Thanh Vân, editors, *Fourth "Rencontres de Blois": Particle Astrophysics*, page 528, Gif sur Yvette, 1992, Editions Frontières
124. A. Bouquet, J. Kaplan, A.L. Melchior, Y. Giraud-Héraud, P. Baillon, in *The Dark Side of the Universe - Experimental Efforts and Theoretical Framework* (1994), pp. 61–68, arXiv:astro-ph/9312009
125. D. Gillieron, AGAPE, internal note, Collège de France, Paris, (1996)
126. J. Kaplan, *Pixel Lensing*, in *Topics on Gravitational Lensing* Napoli Series In Physics and Astrophysics, Bibliopolis (1998)
127. Y. Le Du, Ph.D. thesis, Collège de France, Paris, (2000)
128. R. Ansari, M. Aurière, P. Baillon, et al., Nuclear Physics B Proceedings Supplements **43**, 165 (1995).

A Brief history of the AGAPE group's beginning[9]

The AGAPE collaboration has been formed in the early 1990. The first and original idea of using M31 as a target for microlensing observation is due to P. Baillon. He developed this interest after a seminar given by M. Spiro in 1990 who was then moving, together with J. Rich, the first steps to build the microlensing EROS collaboration. On April 25, 1991, P. Baillon held a seminar at the LPNHE[10] on the possibility to detect microlensing events in M31 using a photomultiplier then in use, Themistocle. Y. Giraud-Héraud was taken by this idea and involved A. Bouquet and J. Kaplan. Even if not yet working on microlensing, they all were aware of the ongoing EROS project. In particular it was soon realised that CCDs were a more suitable instrument to carry out this observational programme. The conclusions of the first preliminar analyses have been presented by P. Baillon in June 1992 (122) and by J. Kaplan in July of the same year (123). A first work was then submitted for a refereed publication in early November 1992 (24). (The authors were not aware of the parallel work carried out by A. Crotts (23), which, still in the pre-arXiv era, had been published only a few days before). The technical aspects for the analysis of the observational data have been developed by A-L. Melchior (124). A key ingredient of the superpixel photometry, the "seeing stabilisation" technique, has been first elaborated by D. Gillieron (125), presented in (126) and then discussed more thoroughly in the PhD thesis of Y. Le Du (127). Finally, the observational campaign was begun in 1994 using the 2m TBL telescope at Pic du Midi, to be continued for further 2 years. Three members of the EROS collaboration, R. Ansari, C. Coutures and M. Moniez, participated in AGAPE, bringing their know how both in observations and in the development of analysis algorithms.

Coming to the name's choice, AGAPE. This comes from a suggestion of A. Bouquet, with an underlying idea of a (friendly) opposition with EROS (a name chosen in opposition to the other microlensing project, MACHO, whose name, on the other hand, had been thought to recall the other dark matter candidate, the WIMP). Indeed, according to the ancient greek mythology, AGAPE/EROS is the couple of holy versus profane love. The right acronym was then found to be "Andromeda Galaxy and Amplified Pixel Experiment". The name AGAPE has been first presented in Stockholm in 1994 par R. Ansari (128).

[9] P. Baillon, A. Bouquet, Y. Giraud-Hèraud, and J. Kaplan, private communication.
[10] Ecole Polytechnique, Palaiseau, France.